POLITECNICO DI TORINO
Repository ISTITUZIONALE

Seismic response of viaducts and bridges isolated with FPS

*Original*
Seismic response of viaducts and bridges isolated with FPS / Miceli, E.. - ELETTRONICO. - 2928:(2023). (Intervento presentato al convegno 7th World Multidisciplinary Civil Engineering-Architecture-Urban Planning Symposium tenutosi a Prague nel 5-9 September 2022) [10.1063/5.0170457].

*Availability:*
This version is available at: 11583/2994364 since: 2024-11-13T10:37:46Z

*Publisher:*
American Institute of Physics - AIP

*Published*
DOI:10.1063/5.0170457

*Terms of use:*

This article is made available under terms and conditions as specified in the corresponding bibliographic description in the repository

*Publisher copyright*

(Article begins on next page)

26 December 2024

AIP Conference Proceedings

RESEARCH ARTICLE | SEPTEMBER 27 2023

# Seismic response of viaducts and bridges isolated with FPS

Elena Miceli

Check for updates

*AIP Conf. Proc.* 2928, 140009 (2023)
https://doi.org/10.1063/5.0170457

View Online
Export Citation
CrossMark

## Articles You May Be Interested In

Specific problems on the use of noise barriers on viaducts

*J Acoust Soc Am* (May 1998)

VISSIM traffic micro-simulation model on Gilingan Viaduct and Gilingan underpass Surakarta

*AIP Conference Proceedings* (June 2018)

Numerical simulation for low frequency noise from viaduct by the vehicle load

*J Acoust Soc Am* (October 2016)

10 October 2023 09:30:59

500 kHz or 8.5 GHz?
And all the ranges in between.
Lock-in Amplifiers for your periodic signal measurements

Find out more
Zurich Instruments

AIP Publishing

# Seismic Response of Viaducts and Bridges Isolated with FPS

Elena Miceli[1, a)]

[1] *Department of Structural, Geotechnical and Building Engineering (DISEG), Politecnico di Torino, Turin, Italy*

[a)] Corresponding author: elena.miceli@polito.it

**Abstract.** This study deals with the evaluation of the seismic isolation of bridges equipped with single concave friction pendulum devices, by comparing the case in which the rigid abutment is present (i.e., multi-span continuous deck bridge) or not (i.e., single column bent viaduct). Two multi degree-of-freedom models are considered for the two cases, while the FPS behaviour is modelled including the velocity dependency. Furthermore, the comparison is carried out by varying the modelling parameters (i.e., pier and deck fundamental period, mass ratio and friction coefficient). The uncertainty in the seismic input is also included by subjecting the two systems to a set of different natural ground motions. The equation of motions are solved in non-dimensional form for both the models in order to obtain the maximum non-dimensional displacement of the substructure. This has led to the evaluation of the optimal sliding friction coefficient able to minimize the maximum non-dimensional pier displacement with the aim of studying the differences between the two numerical models.

10 October 2023 09:30:59

## INTRODUCTION

During the last decades, the safety assessment and maintenance management for infrastructures is becoming very relevant [1]-[3]. The goal of seismic isolation of bridges is to reduce the forces transmitted from the deck to the substructure, i.e., the piers, by increasing the period of the isolation system. During the past years, both the elastomeric and frictional isolators have demonstrated their effectiveness in enhancing seismic performance of structures and infrastructures [4]-[11]. In this context, an isolated three-span continuous deck bridge, equipped with elastomeric bearings, is studied in [12], with the goal to evaluate the bearings peak displacement placed at abutment locations. On the other hand, among the widely adopted isolators, the friction pendulum system (FPS) bearings have the advantage of making the properties of the device independent from the mass deck, which is important in the design phase of the isolator [13]-[15]. In particular, the introduction of the optimal friction coefficient, able to minimize the seismic response of the pier, was first introduced by Jangid in [16]-[17]. In this respect, the optimal friction coefficient is studied in [18] by varying many properties of the structure and the seismic input.

The goal of this work is to evaluate the pier-abutment-deck interaction when bridges are equipped with single concave friction pendulum isolators (FPS). In particular, two six-degree-of-freedom (dofs) models are compared: one representative of a single column bent viaduct (i.e., neglecting the presence of the rigid abutment) and the other for the case of multi-span continuous deck bridge (i.e., including the presence of the abutment). More precisely, for both cases, five dofs are adopted for the lumped masses of the elastic pier and one additional dof representative of the infinitely rigid deck. The equations of motion under a set of seismic inputs are solved for both the models, by performing a non-dimensional analysis. The FPS behaviour is represented by a widespread model that includes the dependency of the friction coefficient from the velocity. Many bridge properties are varied so as to perform a parametric analysis. Then, after having obtained the peak non-dimensional response at the pier level, the optimal sliding friction coefficient, able at minimizing this response, is investigated.

*World Multidisciplinary Civil Engineering-Architecture-Urban Planning Symposium WMCAUS 2022*
AIP Conf. Proc. 2928, 140009-1–140009-10; https://doi.org/10.1063/5.0170457
Published by AIP Publishing. 978-0-7354-4663-2/$30.00

## NON DIMENSIONAL ANALYSIS

To model the seismic response of bridges, both including or neglecting the presence of the rigid abutment, a six-degree-of-freedom (dofs) model is adopted, where 5 dofs are used for the lumped masses of the reinforced concrete (RC) elastic pier, as suggested in [18]-[19], and 1 additional dof is for the infinitely rigid RC deck.

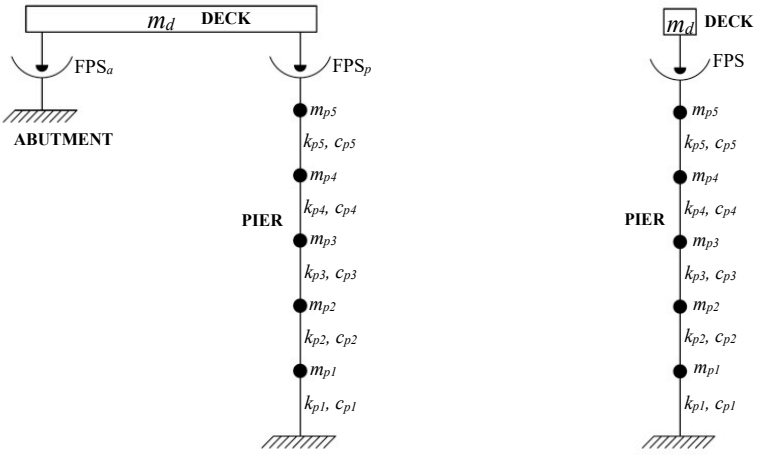


**FIGURE 1.** Six degree-of-freedom models: (a) considering the presence of the rigid abutment; (b) neglecting the presence of the rigid abutment.

Focusing on the case of multi-span continuous deck bridge, where the rigid RC abutment is modelled (Figure 1), subjected to a seismic input along the longitudinal direction, the equation of motion are:

$$
\begin{bmatrix} m_d & m_d & m_d & m_d & m_d & m_d \\ 0 & m_{p5} & m_{p5} & m_{p5} & m_{p5} & m_{p5} \\ 0 & 0 & m_{p4} & m_{p4} & m_{p4} & m_{p4} \\ 0 & 0 & 0 & m_{p3} & m_{p3} & m_{p3} \\ 0 & 0 & 0 & 0 & m_{p2} & m_{p2} \\ 0 & 0 & 0 & 0 & 0 & m_{p1} \end{bmatrix} \cdot \begin{bmatrix} \ddot{u}_d(t) \\ \ddot{u}_{p5}(t) \\ \ddot{u}_{p4}(t) \\ \ddot{u}_{p3}(t) \\ \ddot{u}_{p2}(t) \\ \ddot{u}_{p1}(t) \end{bmatrix} + \begin{bmatrix} c_d & 0 & 0 & 0 & 0 & 0 \\ -c_d & c_{p5} & 0 & 0 & 0 & 0 \\ 0 & -c_{p5} & c_{p4} & 0 & 0 & 0 \\ 0 & 0 & -c_{p4} & c_{p3} & 0 & 0 \\ 0 & 0 & 0 & -c_{p3} & c_{p2} & 0 \\ 0 & 0 & 0 & 0 & -c_{p2} & c_{p1} \end{bmatrix} \cdot \begin{bmatrix} \dot{u}_d(t) \\ \dot{u}_{p5}(t) \\ \dot{u}_{p4}(t) \\ \dot{u}_{p3}(t) \\ \dot{u}_{p2}(t) \\ \dot{u}_{p1}(t) \end{bmatrix} +
$$

$$
+ \begin{bmatrix} \frac{m_d}{2} g / R_p + \frac{m_d}{2} g / R_a & \frac{m_d}{2} g / R_a & \frac{m_d}{2} g / R_a & \frac{m_d}{2} g / R_a & \frac{m_d}{2} g / R_a & \frac{m_d}{2} g / R_a \\ -\frac{m_d}{2} g / R_p & k_{p5} & 0 & 0 & 0 & 0 \\ 0 & -k_{p5} & k_{p4} & 0 & 0 & 0 \\ 0 & 0 & -k_{p4} & k_{p3} & 0 & 0 \\ 0 & 0 & 0 & -k_{p3} & k_{p2} & 0 \\ 0 & 0 & 0 & 0 & -k_{p2} & k_{p1} \end{bmatrix} \cdot \begin{bmatrix} u_d \\ u_{p5} \\ u_{p4} \\ u_{p3} \\ u_{p2} \\ u_{p1} \end{bmatrix} +
$$

$$
+ \begin{bmatrix} \frac{m_d}{2} g \mu_p \left( \dot{u}_d(t) \right) Z(t) + \frac{m_d}{2} g \mu_a \left( \dot{u}_d(t) + \sum_{i=1}^{5} \dot{u}_{pi}(t) \right) Z(t) \\ -\frac{m_d}{2} g \mu_p (\dot{u}_d(t)) Z(t) \\ 0 \\ 0 \\ 0 \\ 0 \end{bmatrix} = +\ddot{u}_g(t) \cdot \begin{bmatrix} -m_d \\ -m_{p5} \\ -m_{p4} \\ -m_{p3} \\ -m_{p2} \\ -m_{p1} \end{bmatrix} \tag{1}
$$

10 October 2023 09:30:59

where $u_d$ is the deck displacement with respect to the pier top, $u_{pi}$ is the displacement of the ith lumped mass of the pier with respect to the lower one, $m_d$ is the mass of the deck, $m_{pi}$ is the mass of the ith lumped mass of the pier, $k_{pi}$ is the corresponding stiffness, $c_d$ and $c_{pi}$ are, respectively, the viscous damping coefficient for the device and for the pier masses, $Z(t)$ indicate the sign function of the velocity, with $t$ the instant of time and the dots indicate differentiation. The resisting forces of the FPS bearings located on top of the abutment and on the pier are, respectively, $F_a(t)$ and $F_p(t)$, expressed as the sum of an elastic component and a viscous component, as follows [15]:

$$\begin{aligned} F_a(t) &= \frac{m_d g}{2}\left[\frac{1}{R_a}\left(u_d(t)+\sum_{i=1}^{5}u_{pi}\right)+\mu_a\left(\dot{u}_d+\sum_{i=1}^{5}\dot{u}_{pi}\right)\mathrm{sgn}\left(\dot{u}_d+\sum_{i=1}^{5}\dot{u}_{pi}\right)\right] \\ F_p(t) &= \frac{m_d g}{2}\left[\frac{1}{R_p}u_d(t)+\mu_p(\dot{u}_d)\mathrm{sgn}(\dot{u}_d)\right] \end{aligned} \tag{2}$$

where the stiffness of the deck is equal to $k_d = W/R = m_d g/R$, half for the bearing on the abutment and half for the pier, the radii of curvature of the FPS bearings are $R_a$ and $R_p$, placed, respectively, on the abutment and on the pier and assumed equal, $g$ is the gravity constant, $\mu$ is the sliding friction coefficient of the bearings. As anticipated, the fundamental period of the deck only depends on the geometrical properties of the isolator, since it is expressed as $T_d = 2\pi\sqrt{m_d/k_d} = 2\pi\sqrt{R/\mathrm{g}}$ [15]. It noteworthy that the two expressions in (2) differ only in terms of displacements, since $F_a(t)$ depends on the relative displacement of the deck with respect to the ground while $F_p(t)$ is function of the deck displacement with respect to the pier top. Regarding the sliding friction coefficient, its dependency on the velocity is such that [20]-[23]:

$$\mu(\dot{u}_d) = f_{\max} - (f_{\max} - f_{\min})\cdot\exp(-\alpha|\dot{u}_d|) \tag{3}$$

where $f_{\max}$ and $f_{\min}$ are the sliding friction parameters at maximum and zero velocity, $\alpha$ is a parameter that controls the transition from low to large velocities. In this work, it is assumed $\alpha$ equal to 30 and $f_{\max} = 3f_{\min}$ [23].

The equation of motions expressed in (1) are then elaborated so as to obtain their nondimensional form, according to the Buckingham's Π-theorem [24]. In particular, a time scale is introduced and assumed equal to $1/\omega_d$, with $\omega_d = \sqrt{\mathrm{k}_d/\mathrm{m}_d}$ indicating the circular frequency of the isolation system. Thus, passing from the time $t$ to $\tau = t\omega_d$, the ground motion input of equation (1) becomes $\ddot{u}_g(t) = a_0 l(t) = a_0 \ell(\tau)$, where $l(t)$ is a nondimensional function of the seismic input time-history over time $t$, while $\ell(\tau)$ contains the same information in the new time $\tau$. In addition, a length scale is introduced equal to $a_0/\omega_d^2$, where $a_0$ is an intensity measure for the seismic input. In the end, dividing the equations in (1) for the deck mass $m_d$ and introducing the time and length scales, the nondimensional equations become:

10 October 2023 09:30:59

$$
\begin{bmatrix} 1 & 1 & 1 & 1 & 1 & 1 \\ 0 & \lambda_{p5} & \lambda_{p5} & \lambda_{p5} & \lambda_{p5} & \lambda_{p5} \\ 0 & 0 & \lambda_{p4} & \lambda_{p4} & \lambda_{p4} & \lambda_{p4} \\ 0 & 0 & 0 & \lambda_{p3} & \lambda_{p3} & \lambda_{p3} \\ 0 & 0 & 0 & 0 & \lambda_{p2} & \lambda_{p2} \\ 0 & 0 & 0 & 0 & 0 & \lambda_{p1} \end{bmatrix} \cdot \begin{bmatrix} \ddot{\psi}_d(\tau) \\ \ddot{\psi}_{p5}(\tau) \\ \ddot{\psi}_{p4}(\tau) \\ \ddot{\psi}_{p3}(\tau) \\ \ddot{\psi}_{p2}(\tau) \\ \ddot{\psi}_{p1}(\tau) \end{bmatrix} +
$$

$$
+ \begin{bmatrix} 2\xi_d & 0 & 0 & 0 & 0 & 0 \\ -2\xi_d & 2\xi_{p5}\frac{\omega_{p5}}{\omega_d}\lambda_{p5} & 0 & 0 & 0 & 0 \\ 0 & -2\xi_{p5}\frac{\omega_{p5}}{\omega_d}\lambda_{p5} & 2\xi_{p4}\frac{\omega_{p4}}{\omega_d}\lambda_{p4} & 0 & 0 & 0 \\ 0 & 0 & -2\xi_{p4}\frac{\omega_{p4}}{\omega_d}\lambda_{p4} & 2\xi_{p3}\frac{\omega_{p3}}{\omega_d}\lambda_{p3} & 0 & 0 \\ 0 & 0 & 0 & -2\xi_{p3}\frac{\omega_{p3}}{\omega_d}\lambda_{p3} & 2\xi_{p2}\frac{\omega_{p2}}{\omega_d}\lambda_{p2} & 0 \\ 0 & 0 & 0 & 0 & -2\xi_{p2}\frac{\omega_{p2}}{\omega_d}\lambda_{p2} & 2\xi_{p1}\frac{\omega_{p1}}{\omega_d}\lambda_{p1} \end{bmatrix} \cdot \begin{bmatrix} \dot{\psi}_d(\tau) \\ \dot{\psi}_{p5}(\tau) \\ \dot{\psi}_{p4}(\tau) \\ \dot{\psi}_{p3}(\tau) \\ \dot{\psi}_{p2}(\tau) \\ \dot{\psi}_{p1}(\tau) \end{bmatrix} +
$$

$$
+ \begin{bmatrix} 1 & 0 & 0 & 0 & 0 & 0 \\ -1 & \lambda_{p5}\frac{\omega_{p5}^2}{\omega_d^2} & 0 & 0 & 0 & 0 \\ 0 & -\lambda_{p5}\frac{\omega_{p5}^2}{\omega_d^2} & \lambda_{p4}\frac{\omega_{p4}^2}{\omega_d^2} & 0 & 0 & 0 \\ 0 & 0 & -\lambda_{p4}\frac{\omega_{p4}^2}{\omega_d^2} & \lambda_{p3}\frac{\omega_{p3}^2}{\omega_d^2} & 0 & 0 \\ 0 & 0 & 0 & -\lambda_{p3}\frac{\omega_{p3}^2}{\omega_d^2} & \lambda_{p2}\frac{\omega_{p2}^2}{\omega_d^2} & 0 \\ 0 & 0 & 0 & 0 & -\lambda_{p2}\frac{\omega_{p2}^2}{\omega_d^2} & \lambda_{p1}\frac{\omega_{p1}^2}{\omega_d^2} \end{bmatrix} \cdot \begin{bmatrix} \psi_d(\tau) \\ \psi_{p5}(\tau) \\ \psi_{p4}(\tau) \\ \psi_{p3}(\tau) \\ \psi_{p2}(\tau) \\ \psi_{p1}(\tau) \end{bmatrix} + \begin{bmatrix} \frac{g\mu(\dot{\psi}_d(\tau))}{a_0}\mathrm{sgn}(\dot{\psi}_d(\tau)) \\ -\frac{g\mu(\dot{\psi}_d(\tau))}{a_0}\mathrm{sgn}(\dot{\psi}_d(\tau)) \\ 0 \\ 0 \\ 0 \\ 0 \end{bmatrix} = +l(\tau) \cdot \begin{bmatrix} -1 \\ -\lambda_{p5} \\ -\lambda_{p4} \\ -\lambda_{p3} \\ -\lambda_{p2} \\ -\lambda_{p1} \end{bmatrix} \tag{4}
$$

where $\psi_d = u_d\omega_d^2/a_0$ and $\psi_{pi} = u_{pi}\omega_d^2/a_0$ are the nondimensional displacements, $\omega_d = \sqrt{k_d/m_d}$ and $\omega_{pi} = \sqrt{k_{pi}/m_{pi}}$ are the circular vibration frequencies, $\xi_d = c_d/2m_d\,\omega_d$ and $\xi_{pi} = c_{pi}/2m_{pi}\,\omega_{pi}$ are the damping factors (respectively for the deck and for the i-th lamped masses of the pier) and $\lambda_p = \lambda_{pi} = m_{pi}/m_d$ is the mass ratio of the i-th lumped mass (all the lumped masses are assumed equal). Hence, the nondimensional parameters Π of the problem are:

$$
\Pi_{\omega_p} = \frac{\omega_p}{\omega_d},\ \ \Pi_{\omega_g} = \frac{\omega_d}{\omega_g},\ \ \Pi_\lambda = \lambda_p,\ \ \Pi_{\xi_d} = \xi_d,\ \ \Pi_{\xi_p} = \xi_{pi},\ \ \Pi_\mu = \frac{\mu(\dot{\psi}_d)g}{a_0} \tag{5}
$$

In the end, to discard the dependency of the nondimensional parameter $\Pi_\mu$ from the velocity, its value is substituted by $\Pi_\mu^* = f_{\max}\,g/a_0$.

Regarding the equations of motion for the case of a single-column bent viaduct (Figure 2), where the abutment is not considered, the nondimensional equation of motion are equal to the ones in (1) and (4), with the only difference that the term relative to $F_a(t)$ is not present.

10 October 2023 09:30:59

## PROBLEM'S PARAMETERS

In this section, the main properties of the problem are discussed. These assumptions are valid both for the case of considering or neglecting the presence of the pier-deck-abutment interaction.

First of all, concerning the seismic input, a set of 30 seismic ground motions is considered, selected from 19 different earthquakes [25]-[27]. The magnitude varies in the range 6.3 to 7.5, the source-to-site distance goes from 13 km to 98 km and the peak ground acceleration is in the range 0.13 - 0.82 g. The intensity measure (IM) [28]-[32], as also previously indicated as the seismic intensity $a_0$, is herein chosen as the spectral pseudo-acceleration $S_A\left(T_d,\xi_d\right)$. Assuming the damping ratio $\xi_d$ equal to zero [33], the spectral pseudo-acceleration becomes only function of the deck fundamental period, meaning that $a_0 = S_A\left(T_d\right)$.

Regarding the structural properties, the damping ratios are set equal to $\Pi_{\xi_d} = \xi_d = 0\%$ and $\Pi_{\xi_p} = \xi_p = 5\%$, the pier period varies from 0.10s to 0.20s, the deck period is in the range 2s-4s, the mass ratio assumes the value 0.1, 0.15, 0.2 and, finally, the normalized friction coefficient is in between 0 and 2.

The equation of motions expressed in (4) are solved for each of the two models by varying the previously mentioned parameters and by considering each of the 30 ground motions, using the Runge-Kutta-Fehlberg integration algorithm available in Matlab-Simulink [34]. For each simulation, the peak normalised response in terms of pier top displacement is numerically calculated and expressed as:

$$\psi_{u_p} = \frac{u_{p,\max}\omega_d^2}{a_0} = \frac{\left(\max\sum_{i=1}^{5} u_{p_i}\right)\omega_d^2}{a_0} \tag{6}$$

Then, the response parameters are probabilistically treated and assumed as lognormally distributed [33],[35]-[37], with geometric mean $GM\left(\psi_{u_p}\right)$ and standard deviation $\beta\left(\psi_{u_p}\right)$ as follows [38]-[47]:

$$GM\left(\psi_{u_p}\right) = \sqrt[N]{\psi_{u_p 1}\cdot\ldots\cdot\psi_{u_p N}} \tag{7}$$

$$\beta\left(\psi_{u_p}\right) = \sqrt{\frac{\left(\ln\psi_{u_p 1} - \ln\left[GM\left(\psi_{u_p}\right)\right]\right)^2 + \ldots + \left(\ln\psi_{u_p N} - \ln\left[GM\left(\psi_{u_p}\right)\right]\right)^2}{N-1}} \tag{8}$$

where $\psi_{u_p j}$ is the j-th realization of the response parameter and *j=1,…,N* with *N=30* the total number of seismic inputs.

## SEISMIC RESPONSE AND OPTIMAL FRICTION COEFFICIENT

In this section, the response of the pier and the optimal friction coefficient results are illustrated. Figure 3 shows, for both the structural systems, the mean value of the maximum normalized pier displacement $GM\left(\psi_{u_p}\right)$ as function of $T_d$ and $\Pi_\mu^*$, for fixed values of $T_p$ and $\lambda$. In general, the mean value decreases for larger values of $T_d$ and of $\lambda$. On the opposite, the response is lower for lower values of pier period. Regarding the dependency on the normalized friction coefficient $\Pi_\mu^*$, it is possible to observe the existence of an optimal value where the response is minimized. Figure 4 presents the same results but in terms of dispersion $\beta\left(\psi_{u_p}\right)$. The dispersion tends to be larger if the pier-abutment-deck interaction is modelled and in general tends to be larger when the optimal value of $\Pi_\mu^*$ is reached and to not be influenced by the other parameters.

10 October 2023 09:30:59

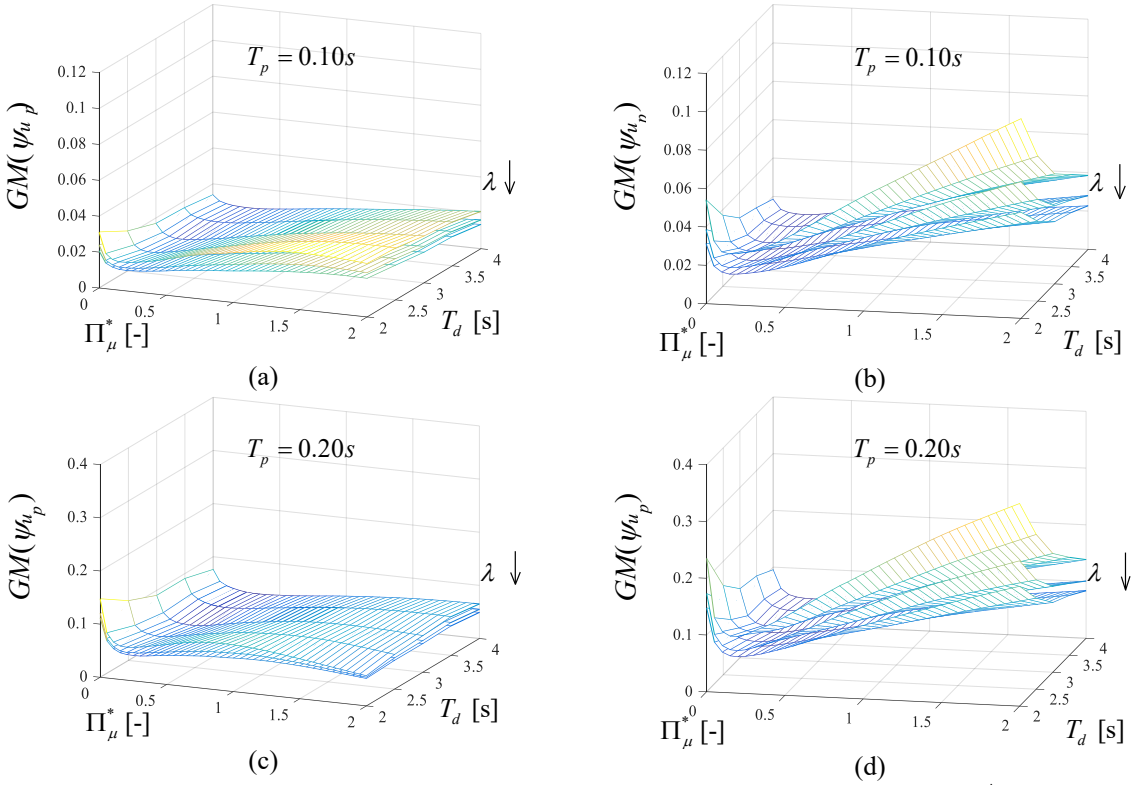


**FIGURE 2.** Median value of the maximum normalized pier displacement as function of $T_d$ and $\Pi^*_\mu$, for fixed values of $T_p$ and $\lambda$ : (a)-(c) considering the presence of the abutment; (b)-(d) neglecting the presence of the abutment

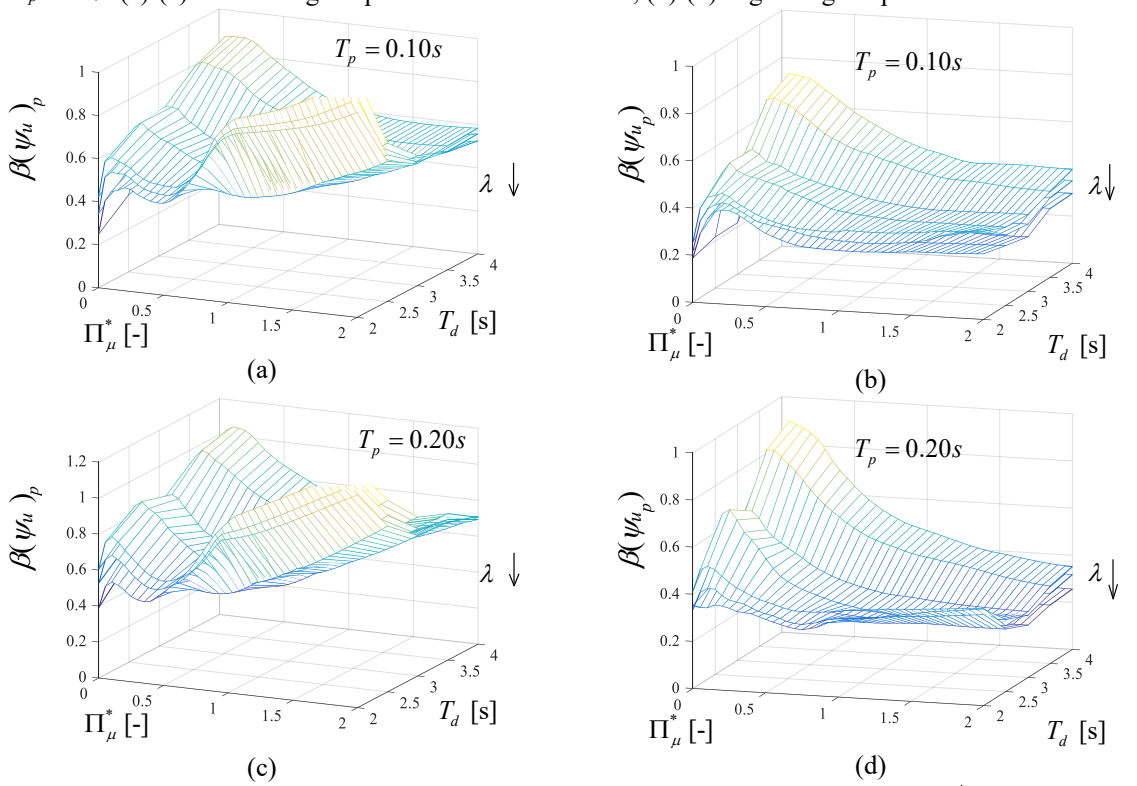


**FIGURE 3.** Dispersion of the maximum normalized pier displacement as function of $T_d$ and $\Pi^*_\mu$, for fixed values of $T_p$ and $\lambda$ : (a)-(c) considering the presence of the abutment; (b)-(d) neglecting the presence of the abutment

10 October 2023 09:30:59

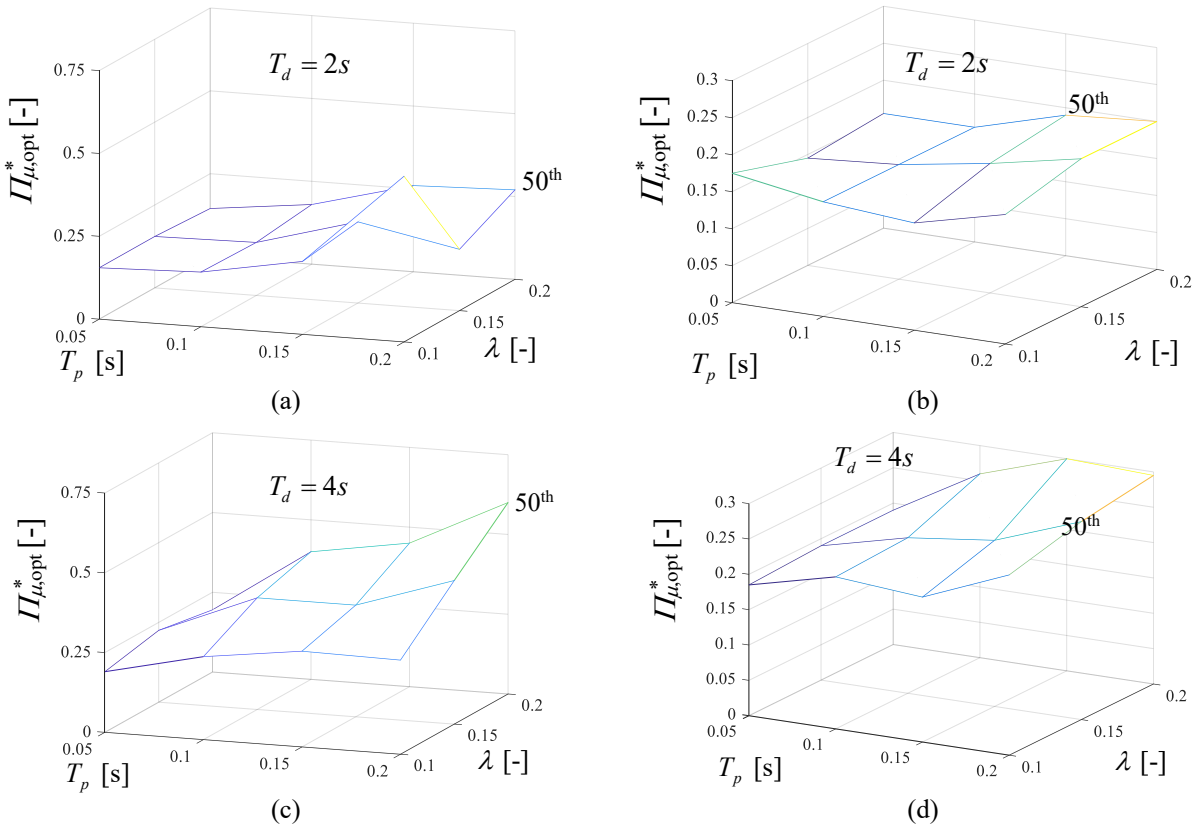


**FIGURE 4.** Optimal friction coefficient as function of $T_p$ and $\lambda$, for fixed values of $T_d$: (a)-(c) considering the presence of the abutment; (b)-(d) neglecting the presence of the abutment

From the previous results, it is possible to observe the existence of an optimal value where the response is minimized. In Figure 4 it is illustrated the optimum of $\Pi^*_\mu$, which is not only function of the parameters involved in the problem (i.e., $T_d$, $T_p$, $\lambda$), but it also depends on the structural system (i.e., if considering or not the presence of the abutment). In particular, the sagging zones of the response as function of $\Pi^*_\mu$ are more pronounced when the interaction with the abutment is not considered, since the bearing on top of the abutment slides faster than the device placed on the pier. Furthermore, when all the structural parameters $\lambda, T_p, T_d$ are considered with their maximum values, larger values of the optimum friction coefficient are required to increase the energy dissipation.

Finally, it is important to highlight that any numerical model is always characterized by uncertainties that influence the numerical simulations and so the safety assessment, as discussed in [48]-[58].

## CONCLUSION

This work analyses the seismic performance of bridges isolated with single concave friction pendulum bearings, focusing on the pier-abutment-deck interaction. In particular, two six-degree-of-freedom structural systems are modelled: one including the presence of the abutment (i.e., multi-span continuous deck bridge) and another neglecting its presence (i.e., single-column bent viaduct). Different values for the main problem parameters are considered within a parametric analysis and the uncertainty in the seismic input is included by considering a set of 30 natural ground motions. The equations of motions are numerically solved in a non-dimensional form so as to evaluate the maximum normalized response of the pier. This response tends to first decrease and then increase as function of the normalized friction coefficient of the bearing. When the presence of the abutment is considered (i.e., multi-span continuous deck bridge), this minimum value is less pronounced, since the bearing on top of the abutment tends to slide faster than the one on the pier. The existence of a minimum value for the pier response has

10 October 2023 09:30:59

suggested to evaluate an optimal value for the normalized friction coefficient, as function of the other parameters involved. In the case multi-span continuous deck bridge, higher optimal values are observed.

## REFERENCES


1. R. Troisi and G. Alfano, "Towns as Safety Organizational Fields: An Institutional Framework in Times of Emergency", Sustainability **11**(24), 7025 (2019). DOI:10.3390/su11247025.
2. R. Troisi and L. Arena, "Organizational Aspects of Sustainable Infrastructure Safety Planning by Means of Alert Maps", Sustainability (Switzerland) **14**(4), 2335 (2022).
3. R. Troisi and P. Castaldo, "Technical and organizational challenges in the risk management of road infrastructures", J. Risk Res., (2022). DOI:10.1080/13669877.2022.2028884.
4. M. C. Constantinou, A. Kartoum, A. M. Reinhorn and P. Bradford, "Sliding isolation system for bridges: Experimental study", Earthq. Spectra **8**(3), 321-344 (1992).
5. A. Kartoum, M. C. Constantinou and A. M. Reinhorn, "Sliding isolation system for bridges: Analytical study", J. Struct. Eng. **8**(3), 345-372 (1992).
6. P. Tsopelas, M. C. Constantinou, Y. S. Kim and S. Okamoto, "Experimental study of FPS system in bridge seismic isolation", Earthq. Eng. Struct. Dyn. **25**(1), 65-78 (1996a).
7. A. Ghobarah and H. M. Ali, "Seismic performance of highway bridges", Eng. Struct. **10**(3), 157-166 (1988).
8. M. Dicleli and S. Buddaram, "Effect of isolator and ground motion characteristics on the performance of seismic-isolated bridges", Earthq. Eng. Struct. Dyn. **35**(2), 233-250 (2006).
9. P. Tsopelas, M. C. Constantinou, S. Okamoto, S. Fujii and D. Ozaki, "Experimental study of bridge seismic sliding isolation systems", Eng. Struct. **18**(4), 301-310 (1996).
10. R. S. Jangid, "Seismic Response of Isolated Bridges", J. Bridge Eng. **9**(2), 156-166 (2004).
11. R. S. Jangid, "Equivalent linear stochastic seismic response of isolated bridges", J. Sound Vib. **309**(3-5), 805-822 (2008).
12. N. P. Tongaonkar and R. S. Jangid, "Seismic response of isolated bridges with soil–structure interaction", Soil Dyn. Earthq. Eng. **23**, 287–302 (2003).
13. L. Su, G. Ahmadi and I. G. Tadjbakhsh, "Comparative study of base isolation systems", J. Eng. Mech. **115**(9), 1976–92 (1989).
14. Y. P. Wang, L. L. Chung and W. H. Liao, "Seismic response analysis of bridges isolated with friction pendulum bearings", Earthq. Eng. Struct. Dyn. **27**, 1069-1093 (1998).
15. V. A. Zayas, S. S. Low and S. A. Mahin, "A simple pendulum technique for achieving seismic isolation", Earthq. Spectra **6**(2), 317–33 (1990).
16. R. S. Jangid, "Optimum frictional elements in sliding isolation systems", Comput. Struct. **76**(5), 651–661 (2000).
17. R. S. Jangid, "Optimum friction pendulum system for near-fault motions", Eng. Struct. **27**(3), 349–359 (2005).
18. P. Castaldo and G. Amendola, "Optimal DCFP bearing properties and seismic performance assessment in nondimensional form for isolated bridges", Earthq. Eng. Struct. Dyn. **50**(9), 2442–2461 (2021).
19. P. Castaldo and G. Amendola, "Optimal Sliding Friction Coefficients for Isolated Viaducts and Bridges: A Comparison Study", Struct. Control Health Monit. **28**(12), e2838, (2021).
20. A. Mokha, M. C. Constantinou and A. M. Reinhorn, "Teflon Bearings in Base Isolation. I: Testing", J. Struct. Eng. **116**(2), 438-454 (1990).
21. M. C. Constantinou, A. Mokha and A. M. Reinhorn, "Teflon Bearings in Base Isolation. II: Modeling", J. Struct. Eng. **116**(2), 455-474 (1990).
22. R. S. Jangid, "Computational numerical models for seismic response of structures isolated by sliding systems", Struct. Control Health Monit. **12**, 117–137 (2005).
23. M. C. Constantinou, A. S. Whittaker, Y. Kalpakidis, D. M. Fenz and G. P. Warn, "Performance of Seismic Isolation Hardware Under Service and Seismic Loading", Technical Report MCEER-07-0012, (2007).
24. N. Makris and C. J. Black, "Dimensional analysis of inelastic structures subjected to near fault ground motions", Technical report EERC 2003/05, (2003).
25. PEER, Pacific Earthquake Engineering Research Center http://peer.berkeley.edu/.
26. ITACA, Italian Accelerometric Archive http://itaca.mi.ingv.it/ItacaNet/itaca10_links.htm.


10 October 2023 09:30:59

27. ISESD, Internet-Site for European Strong-Motion Data http://www.isesd.hi.is/ESD_Local/frameset.htm.
28. H. Aslani and E. Miranda, "Probability-based seismic response analysis", Eng. Struct. **27**(8), 1151-1163 (2005).
29. M. De Iuliis and P. Castaldo, "An energy-based approach to the seismic control of one-way asymmetrical structural systems using semi-active devices", Ing. Sism. **29**(4), 31-42 (2012).
30. P. Castaldo and M. De Iuliis, "Optimal integrated seismic design of structural and viscoelastic bracing-damper systems", Earthq. Eng. Struct. Dyn **43**(12), 1809–1827 (2014).
31. B. Palazzo, P. Castaldo and I. Marino, "The dissipative column: A new hysteretic damper", Buildings **5(**1), 163-178 (2015).
32. K. A. Porter, "An overview of PEER's performance-based earthquake engineering methodology," in *Civil Engineering*, Proceedings of the 9th International Conference on Application of Statistics and Probability (ICASP9, San Francisco, California, 2003).
33. K. Ryan and A. Chopra, "Estimation of Seismic Demands on Isolators Based on Nonlinear Analysis", J. Struct. Eng. **130**(3), 392-402 (2004).
34. Math Works Inc., MATLAB-High Performance Numeric Computation and Visualization Software. User's Guide (Natick, MA, USA, 1997).
35. P. Castaldo and M. Ripani, "Optimal design of friction pendulum system properties for isolated structures considering different soil conditions", Soil Dyn. Earthq. Eng. **90**, 74–87 (2016).
36. P. Castaldo, B. Palazzo, T. Ferrentino and G. Petrone, "Influence of the strength reduction factor on the seismic reliability of structures with FPS considering intermediate PGA/PGV ratios", Compos. B. Eng. **115**, 308-315 (2017).
37. P. Castaldo, B. Palazzo and T. Ferrentino, "Seismic reliability-based ductility demand evaluation for inelastic base-isolated structures with friction pendulum devices", Earthq. Eng. Struct. Dyn **46**(8), 1245-1266 (2017).
38. R. Troisi and G. Alfano, "Firms'crimes and land use in Italy. An exploratory data analysis", Smart Innov. Syst. Technol. **178**, 749–758 (2020).
39. C. Garzillo and R. Troisi, "Le decisioni dell'EMA nel campo delle medicine umane. In EMA e le relazioni con le Big Pharma - I profili organizzativi della filiera del farmaco", in G. Giappichelli, pp. 85-133 (2015).
40. L. E. Golzio and R. Troisi, "The value of interdisciplinary research: a model of interdisciplinarity between legal re-search and research in organizations", J. Dev. Leadersh. **2**, 23-38 (2013).
41. A. Nese and R. Troisi, "Corruption among mayors: evidence from Italian Court of Cassation judgments. Trends Organ. Crime **22**(3), 298-323 (2019).
42. R. Troisi and L.E. Golzio, "Legal studies and organization theory: a possible cooperation," in *European Academy of Management*, 16th EURAM Conference Manageable cooperation (Paris, 1-4 June 2016), pp. 1-23.
43. R. Troisi and V. Guida, "Is the Appointee Procedure a Real Selection or a Mere Political Exchange? The Case of the Italian Health-Care Chief Executive Officers", J. Entr. Organ. Div. **7**(2), 19-38 (2018). DOI:10.5947/jeod.2018.008.
44. R. Troisi, "Le risorse umane nelle BCC: lavoro e motivazioni al lavoro" in *Progetto aree bianche. Il sistema del credito cooperativo in Campania* **1**, edited by Ecra (Roma, 2012), pp. 399-417.
45. R. Troisi and G. Alfano, "Is regional emergency management key to containing COVID-19? A comparison between the regional Italian models of Emilia-Romagna and Veneto", Int. J. Public Sect. Manag. 35(2), 195-210 (2021). DOI: 10.1108/IJPSM-06-2021-0138.
46. R. Troisi, P. Di Nauta and P. Piciocchi, "Private corruption: An integrated organizational model", Eur. Manag. Rev., 1-11 (2021).
47. A. Nese and R. Troisi, "Individual Preferences and Job Characteristics: An Analysis of Cooperative Credit Banks", Labour **28**(2), 233–249 (2014).
48. P. Castaldo, D. Gino, G. Marano and G. Mancini, "Aleatory uncertainties with global resistance safety factors for non-linear analyses of slender reinforced concrete columns", Eng. Struct. **255**(1), 113920 (2022).
49. P. Castaldo, E. Nastri and V. Piluso, "Ultimate behaviour of RHS temper T6 aluminium alloy beams subjected to non-uniform bending: Parametric analysis", Thin-Walled Struct. **115**, 129–141 (2017).
50. P. Castaldo, E. Nastri and V. Piluso, "FEM simulations and rotation capacity evaluation for RHS temper T4 aluminium alloy beams", Compos. B. Eng. **115**, 124-137 (2017).

10 October 2023 09:30:59

51. G. Bertagnoli, L. Giordano and S. Mancini, “A metaheuristic approach to skew reinforcement optimization in concrete shells under multiple loading conditions”, Struct. Eng. Int.: J. Int. Assoc. Bridge Struct. Eng. (IABSE) **24**(2), 201–210 (2014).
52. L. Giordano and G. Mancini, “Fatigue behaviour simulation of bridge deck repaired with self compacting concrete”, J. Adv. Concr. Technol. **7**(3), 415–424 (2009).
53. G. Bertagnoli, L. Giordano and S. Mancini, “Optimization of concrete shells using genetic algorithms”, Z. Angew. Math. Mech. (ZAMM) **94**(1-2), 43–54 (2014).
54. G. Bertagnoli and V.I Carbone, “A finite element formulation for concrete structures in plane stress”, Struct. Concr. **9**(2), 87–99 (2008).
55. G. Bertagnoli, D. Gino and G. Mancini, “Effect of endogenous deformations in composite bridges,” in *Progress in Steel and Composite Structures,* Proceedings of the 13th International Conference on Metal Structures ICMS, 287–298 (2016).
56. G. Bertagnoli, G. Mancini and F. Tondolo, “Numerical modelling of early-age concrete hardening”, Mag. Concr. Res. **61**(4), 299–307 (2009).
57. D. Gino, P. Castaldo, L. Giordano and G. Mancini: “Model uncertainty in non-linear numerical analyses of slender reinforced concrete members”, Struct. Concr. **22**(2), 845–870 (2021).
58. D. Gino, P. Castaldo, G. Bertagnoli, L. Giordano and G. Mancini, “Partial factor methods for existing structures according to fib Bulletin 80: Assessment of an existing prestressed concrete bridge”, Struct. Concr. **21**(1), 15–31 (2020).

10 October 2023 09:30:59